Please cite: *Chang T-J, Wang C-H, Chen AS, Djordjevic S (2018) The effect of inclusion of inlets in dual drainage modelling, Journal of Hydrology. (In press)* 10.1016/j.jhydrol.2018.01.066

The effect of inclusion of inlets in dual drainage modelling

Tsang-Jung Chang[1,2], Chia-Ho Wang[1], Albert S. Chen[3,*], Slobodan Djordjević[3]

[1] Department of Bioenvironmental Systems Engineering, National Taiwan University, Taipei, Taiwan
[2] Hydrotech Research Institute, National Taiwan University, Taipei, Taiwan
[3] Centre for Water Systems, College of Engineering, Mathematics and Physical Sciences, University of Exeter, Exeter, United Kingdom

Abstract

In coupled sewer and surface flood modelling approaches, the flow process in gullies is often ignored although the overland flow is drained to sewer network via inlets and gullies. Therefore, the flow entering inlets is transferred to the sewer network immediately, which may lead to a different flood estimation than the reality. In this paper, we compared two modelling approach with and without considering the flow processes in gullies in the coupled sewer and surface modelling. Three historical flood events were adopted for model calibration and validation. The results showed that the inclusion of flow process in gullies can further improve the accuracy of urban flood modelling.

Keywords: Coupled 1D/2D flood model; Dynamic flow interaction; Model comparison; Overland flow; Roof drainage; Storm sewer flow.

1 Introduction

Flooding is a major hazard in many urban areas that leads to significant damage to properties and disruption of services. Hydraulic modelling is the key for better understanding of flood dynamic such that enhanced adaptation measures can be applied for disaster risk reduction (DRR). For most modern cities, storm sewer networks are built to manage surface water caused by local rainfall. However, the cost for the construction and maintenance of drainage networks is expensive such that a standard between 1 in 1 to 1 in 30 years (Balmforth et al., 2006; Bloomberg

and Strickland, 2012; BSI, 2008; CIWEM UDG, 2016) is often used for designing sewer systems. To evaluate the consequence of flooding due to extreme weather conditions that are beyond the design standard, one-dimensional (1D) sewer flow models (SFMs) are widely adopted to examine the performance of drainage systems for dealing with intense rainfall (Arnbjerg-Nielsen, 2008; Rossman, 2010).

To better describe the movement of surcharge flow from sewer networks, instead of using simplified depth-volume functions, overland flow models (OFMs) are introduced to simulate the runoff dynamic on the ground surface. The approach coupling of SFM and OFM is regarded as the Dual Drainage approach (Djordjević et al., 1999) that can be either a combination of 1D SFM and 1D OFM (Leandro et al., 2009), or a combination of 1D SFM and two-dimensional (2D) OFM (Chen et al., 2007; Hsu et al., 2002). Each of these approaches has advantages and disadvantages (Allitt et al., 2009). In the last decade, coupled 1D SFM and 2D OFM have been widely applied to urban flood modelling (Jahanbazi and Egger, 2014; Russo et al., 2015; Seyoum et al., 2012; Vojinovic and Tutulic, 2009). Recently, Leandro and Martins (2016) coupled 2D OFM with 1D SFM (SWMM 5.1) using dynamic link libraries that avoids changing the source code in SWMM. Martins et al. (2017) compared three approaches that were all coupled to the same 1D SFM to analyse the differences in modelling results using the full shallow water equations, the local inertial equations and the diffusive wave equations as the 2D OFM.

In our previous study (Chang et al., 2015), we compared six combinations of 1D SFM and 2D OFM in urban flood modelling, including (1) 2D OFM only; (2) 2D OFM with rainfall reduction or infiltration rate; (3) Combined SFM/OFM; (4) Coupled SFM/OFM; (5) Coupled OFM/SFM; and (6) Mixed SFM/OFM and OFM/SFM coupling. Details of these modelling approaches are provided in Chang et al. (2015).

The results showed that the bidirectional interaction between the sewer network and the ground surface must be included in modelling to provide more accurate estimations (i.e. approaches (4)-(6)). Furthermore, the interaction between the two systems may vary because different land cover conditions have different mechanisms. For example, if rainfall on a flat roof is collected and drained directly to the sewer network then the downstream network may surcharge due to high discharge into the system and the coupled SFM/OFM approach is adequate to simulate the condition that the sewer flow returns to the surface. On the other hand, the excess runoff from the precipitation falling on pervious area may propagate along terrain until reaching an inlet that drains the overland flow into the sewer system, which is better reflected by the coupled OFM/SFM approach. For coping with real-world problems that are often a combination of these two situations, the Mixed SFM/OFM and OFM/SFM coupling was therefore developed as a solution (Chang et al., 2015).

Sewer inlets are the main interface introducing surface runoff into underground drainage network. Nevertheless, in hydraulic modelling, this process is often simplified or neglected because the details of input data required. The recent improvement of data availability has enabled the possibility to analyse the flow behaviour through inlets and their influence in flood modelling. Shepherd et al. (2012) assess the performance of road gullies through a systematic numerical modelling. Bazin et al. (2014) and Chen et al. (2016) investigated how the flow regime through inlet and manhole changes under different flow conditions and proposed a set of methods to calculate the discharge. Djordjević et al. (2012) and Martins et al. (2014) adopted the Computational Fluid Dynamics (CFD) model OpenFOAM to simulate the flow interaction through a gully, which was compared to

laboratory measurements (different laboratory gullies and OpenFOAM settings were employed in these two studies). Gomez et al. (2016) compared the numerical modelling results, using Flow-3D, with the experimental data to evaluate the inlet coefficient. Lopes et al. (2016) also adopted similar approach to estimate the efficiency of gully with grate slots.

In this study, we developed an innovative approach to better simulate the function of inlets during flood events, which was compared to the above-mentioned methods against the measurements in both underground and overland systems of three historical events. The models were calibrated and validated via three flood events with different attributes, i.e. constant moderate rainfall with long duration, intense rainfall with short duration, and extreme rainfall with short duration. The results showed the need to incorporate the new methodology to further improve of modelling accuracy in the Mixed SFM/OFM and OFM/SFM coupling approach.

2 Methodology

2.1 2D OFM

We adopted and 2D non-inertia OFM to simulate the flood propagation on the ground surface. The 2D OFM is coupled with the Storm Water Management Model (SWMM; Huber and Dickinson, 1988) version 4.4 to simulate the bidirectional interactions between the overland and the sewer systems. Both 2D OFM and SWMM4.4 are developed in Fortran hence they are coupled and compiled as a single code. Assuming the local and convective accelerations are small compared with the gravity and friction terms, the acceleration terms in the SWEs are neglected in the governing equations of the 2D OFM:

$$\frac{\partial d}{\partial t}+\frac{\partial ud}{\partial x}+\frac{\partial vd}{\partial y}=q_s\left(x,y,t\right)-q_i\left(x,y,t\right) \tag{1}$$

$$-\frac{\partial h}{\partial x}=S_{fx}+\frac{\left[q_s\left(x,y,t\right)\right]u}{gd} \tag{2}$$

$$-\frac{\partial h}{\partial y}=S_{fy}+\frac{\left[q_s\left(x,y,t\right)\right]v}{gd} \tag{3}$$

101 where,

d : water depth [m];

t : time [s];

u : velocity component in the *x* direction [m/s];

v : velocity components in the *y* direction [m/s];

$h=d+z$: water surface elevation [m];

$S_{fx}=\frac{n^2u\sqrt{u^2+v^2}}{d^{4/3}}$: friction slope in *x* directions [-];

$S_{fy}=\frac{n^2v\sqrt{u^2+v^2}}{d^{4/3}}$: friction slope in *y* direction [-];

n : surface roughness coefficient;

$q_s\left(x,y,t\right)$: discharge rate per unit area that the sewer flow surcharges to ground surface [$m^3/s/m^2$], considered as point source and determined as

$$q_s\left(x,y,t\right)=I+\sum_k\left[\frac{Q_s\left(x_k,y_k,t\right)}{A_s\left(x_k,y_k\right)}\right]\delta\left(x-x_k,y-y_k\right) \tag{4}$$

$q_i\left(x,y,t\right)$: discharge rate per unit area that surface water drains to sewer network [$m^3/s/m^2$], considered as point sink and determined as

$$q_i\left(x,y,t\right)=\sum_k\left[\frac{Q_i\left(x_k,y_k,t\right)}{A_i\left(x_k,y_k\right)}\right]\delta\left(x-x_k,y-y_k\right) \tag{5}$$

I : rainfall excess intensity [m/s];

$Q_s\left(x_k,y_k,t\right)$: surcharge discharge determined by SWMM [m^3/s];

$Q_i(x_k, y_k, t)$: drainage discharge to be added to SWMM as the inflow to an inlet of manhole [m^3/s];

$A_s(x_k, y_k)$: distributed area of surcharge at the point (x_k, y_k) [m^2];

$A_i(x_k, y_k)$: catchment area for inlet at the point (x_k, y_k) [m^2];

δ : Dirac delta function

In Eqs. (2) and (3), it is assumed that the influx direction of rainfall or manhole effluent is perpendicular to the overland surface and the inlet drainage leaves with overland flow velocity components u and v (Abbott and Minns, 1998). The unknowns d, u and v in Eqs. (1) to (3) are solved by an Alternating Direction Explicit scheme. The derivation of finite difference method for the 2D OFM was depicted in Hsu et al. (2000).

2.2 Interaction between OFM and SFM without gullies

As mentioned earlier, we have developed six approaches in an earlier study of urban flood modelling (Chang et al., 2015). Two of the approaches only involve with 2D OFM and no interaction with 1D SFM is considered. The combined SFM/OFM approach runs the 1D SFM to determine the surcharge discharges from the sewer network, which are used as point sources in the 2D OFM. This is a unidirectional interaction where the surface runoff cannot return to the sewer even when the drainage capacity is available.

For the coupled SFM/OFM or OFM/SFM approaches, the interaction between the SFM and OFM is bidirectional such that the runoff can move between the sewer network and the ground surface through manholes or inlets, depending on flow conditions between the two systems. For surcharging condition when the water level in a manhole reaches the ground elevation, the overflow from the sewer network to the ground surface will occur. The discharge from manhole $Q_s(x_k, y_k, t)$ is calculated

by the EXTRAN module in the SWMM and assumed to be distributed uniformly in the adjacent area $A_s(x_k, y_k)$ around location (x_k, y_k) and captured by the overland flow model.

On the other hand, an inlet at location (x_k, y_k) on the ground surface may collect water from its neighbouring area $A_i(x_k, y_k)$ and drain it to the sewer network through the manhole junction that it is connected to. The drainage capacity $Q_d(x_k, y_k)$ of an inlet depends on its type, e.g., if it is a curb-opening inlet, gutter inlet or grated inlet (Mays, 2011). For low flow rate conditions in both the surface and the sewer systems, the overland flow usually drains fully up to the drainage capacity of the inlet. Hence, the inlet discharge $Q_i(x_k, y_k, t)$ is expressed as follow,

$$Q_i(x_k, y_k, t) = \min\left[A_i(x_k, y_k) \frac{\partial d(x_k, y_k, t)}{\partial t}, Q_d(x_k, y_k) \right] \quad (6)$$

where, $d(x_k, y_k, t)$ is water depth [m] at location (x_k, y_k) and time t, $Q_d(x_k, y_k)$ is the design capacity [m^3/s] of the inlet at location (x_k, y_k), which is a given constant. If the manhole that the inlet connects to is not surcharged, the water in the neighbouring area $A_i(x_k, y_k)$ drains with the rate $Q_i(x_k, y_k, t)$ given by Eq. (6). Else, if the manhole is surcharged, which implies that the water is flowing to overland instead of entering sewer, the inlet discharge $Q_i(x_k, y_k, t)$ is set to zero.

2.3 Interaction between OFM and SFM with gullies

In the aforementioned coupled SFM/OFM or OFM/SFM approaches, we simplified the flow dynamic between inlets and manhole, assuming flow transferring from an inlet to a manhole instantly, and the flow interaction between SFM and OFM depends on the flow condition at the manhole. Nevertheless, inlets are connected to

manholes via gullies in reality and the simplification may not reflect the physical phenomena accurately. In this study, we considered the influence of gullies and built a more detailed model with inlets and gullies correctly positioned and connected. As a result, in most conditions the flow exchange between SFM and OFM can only take place at inlets. The only exception is when the high pressure in the sewer network displaces of a manhole cover, thus removing the obstacle for the SFM and OFM flow interaction An innovative approach for dealing with various flow situations related to manhole cover displacement has been developed by Chen et al. (2016).

3 Model applications and comparison

3.1 Case study

In this paper, we aimed to compare the two Mixed SFM/OFM and OFM/SFM coupling approaches, i.e. without and with considering the flow process in gullies (as Model A and Model B shown in Figure 1, respectively), and discuss their suitability in modelling practices. We selected the Datong District, a low-lying area in the northwest part of Downtown Taipei, as the case study. The area is located close to the junction where the Keelung River and the Tamsui River meet. Most of the area has an elevation below 5 m above mean sea level, as shown in Figure 2, and the terrain gradually declines from southeast to west, with an average slope of 0.7%. Flood levees on the west side, along the Tamsui River, and on the north side, along the Keelung River, protect the Downtown Taipei from fluvial flooding. The elevated motorway passing the northeast corner of the district forms a closed boundary that connects the two levees along the Tamsui and Keelung Rivers. The area is highly developed, as shown in Figure 3, with 42% covered by buildings, 28% by roads, 17% as public open space, and only 13% as green areas. We used a 4m resolution

digital elevation, with a total of 400,000 cells, and a 0.5s time step for 2D OFM, while 1s time step was used for 1D SFM.

Figure 4 shows the four storm water drainage networks within the area, including 1,367 manholes and 29.5 km of pipes, that can cope with intense rainfall up to 1 in 5 year return period. Apart from the one (Network 3) in the northwest, the other three (Networks 1, 2 and 4) are connected via three pipes A, B, and C, that allow overflowing from one network to another for easing the burden of the network during extreme conditions.

Sluice gates are installed at the outlets of drainage networks that allow for gravity drainage. If the water level in the Tamsui or the Keelung River stops drainage by gravity, the pumping stations are switched on to exclude the storm water to avoid backwater building up in the sewer network(s). The total pumping capacity of the four stations is substantial. Each pumping station has multiple pumps that are operated automatically based on the outer water level in the river and the inner water level at the detention pool. If the outer water level is higher than the inner water level that prevents gravity drainage, pump(s) will be switched on to discharge the sewer flow into the rivers. The number of pumps in operation depends on the water level in the detention pool.

The rainfall observations from the Taiping Elementary School (TES) rain gauge, as shown in Figure 4, and the water level records at the network outlets and the water level (WL) gauge in the centre of the whole catchment were used for model calibration and validation. The water level at the network outlets included the river water levels and the ones at the detention pools next to the pumping stations.

3.2 Flood events

We collected the records of three recent events in 2015 (i.e. 19 July, 23 July and 7-8 August) in the case study area for model calibration and validation. We adopted the observations at the TES rain gauges as the rainfall inputs, and the river water levels at the outlets of pumping stations as the downstream boundary conditions. The water level records at the WL gauge and the detention pools were used for calibration and validation. The operation rules of pumping stations, including the start and stop levels of each pump, were applied in the modelling to switch pumps on and off automatically. The modelled hydrographs at the detention pools and the WL gauge were compared to the observed data and evaluated using the Nash-Sutcliffe Efficiency (NSE; Nash and Sutcliffe, 1970). We also adopted the indicators Accuracy, Sensitivity and Precision that were defined as functions of True Positive (TP), False Positive (FP), False Negative (FN) and True Negative (TN) to compare the performance of modelling in terms of overland flood extents. More detailed explanation can be found in Cheng et al. (2015).

$$Accuracy = \frac{TP + TN}{TP + TN + FP + FN} \tag{7}$$

$$Sensitivity = \frac{TP}{TP + FN} \tag{8}$$

$$Precision = \frac{TP}{TP + FP} \tag{9}$$

The 7-8 August 2015 event was caused by Typhoon Soudelor that brought in 257mm rainfall within 16 hours, as shown in Figure 5(a). The inner water levels started to increase in all four networks after 23:00 on 7 August when the rainfall began. The outer water levels in river channels exceeded the inner water levels at the outlets of Networks 3 and 4 around 01:00, which stopped drainage by gravity and the pumping stations were switched on to discharge the flow from the sewer

networks to the rivers. The outer water levels increased above the inner water levels at outlets of Network 1 and 2 around 1:50 and 02:20, respectively, when the pumps began to work at these two stations. The prolonged precipitation resulted in high flow rates in sewer pipes, which were close to their full capacity in most part of the network, and a minor flooding was reported at one location. However, no detail regarding the flood extent or depth was available. The flow situation of this event was in-between the other two events, and only a minor surface flooding occurred such that the event was used for model calibration.

The convective rainfall event on 19 July 2015 dumped 23mm rainfall in the case study area, while 15.5 mm concentrated within 20 minutes as shown in Figure 6(a). The rainfall intensity was below the design rainfall 78.5 mm/h so the sewer networks were able to convey runoff without operating the pumping stations.

On 23 July 2015, the area was hit by another storm that brought 125 mm rainfall within 2 hours, as shown in Figure 7(a), with 62 mm concentrated during the peak 30 minutes. The sewer networks were unable to cope with such intense rainfall and flooding occurred in several locations. Both events, which represent moderate and extreme conditions, respectively, have complete water level records at the outlets and the WL gauge in the sewer networks so that we adopted the records to validate the modelling results.

3.3 Modelling results

3.3.1 Model calibration

The modelled water levels at the detention pools of network outlets and the WL gauge using the two Mixed SFM/OFM and OFM/SFM coupling approaches, i.e. (Model A) and (Model B) without and with considering the flow processes in gullies, respectively, of the 7-8 August 2015 event are compared to the observation records

in Figure 8. The peak water levels at the WL gauge were following the peaks of the change of rainfall intensity. The results from both Models A and B captured the trend properly with only slight overestimation during the peaks.

The water levels in the detention pools at the outlets from both models were very similar for all four networks. The water level at Network 4 outlet (Figure 8 (e)) varied almost simultaneously with the changes of rainfall intensity with a 10 to 15 minutes delay because the catchment is relatively small and the location of the outlet is very close to the TES gauge. The river water level quickly rose above the water level in the detention pool such that the pump operation played an important role in managing the water level. Four pumps were switched on when the water level at the pool exceeded 0.95m, 0.97m, 1.0m, and 1.02m, respectively. The pumps were operating until the water level reduced to 0.18m, 0.31m, 0.31m and 0.35m, respectively. When the pumps were running, the water level at the pool was dominated by the operation of pumps rather than the rainfall. The same conditions apply to the water level hydrograph at the Network 3 outlet pool (Figure 8 (d)).

Due to the larger catchment areas and the longer distances of main trunks, the water levels at outlets of Networks 1 and 2 varied less significantly with the changes of rainfall intensity than the ones in Networks 3 and 4. The water level at Network 1 outlet pool (Figure 8 (b)) increased until 01:50, when the river water level exceeded than the pool water level so the pump station began operation. After 05:00, the water level dropped quickly as the result of reduced rainfall and the continuous operation of the pumping station. Similar responses can be found at the Network 2 outlet pool (Figure 8 (c)). The water level changes at the WL gauge (Figure 8 (a)) and the variation of the hydrograph at the Network 2 outlet pool (Figure 8 (c)) show the backwater effect from the downstream. Therefore, the relationship between the

rainfall intensity and the water level at the WL gauge was not obvious. The parameters to be calibrated were the roughness in both the 2D OFM and the 1D SFM. The parameters were adjusted, based on land cover types, and pipe diameters and slopes, and calibrated until the modelled water level hydrographs at all locations were consistent with the observed ones, i.e. NSE was close to 1. The roughness values were determined as (1) 0.02 for roads, plazas, pavements, etc.; (2) 0.08 for green lands, parks, etc.; and (3) 0.05 for built-up areas. The range of roughness of pipes was 0.013-0.018.

In general, Model A predicted slightly higher water level than Model B did, especially for the peak values. The NSEs shown in Table 1 indicate that Model B performed better than Model A for the WL gauge and all networks.

3.3.2 Model validation

Figure 9 compares the observed and modelled water level hydrographs at the network outlets and the WL gauge of 19 July 2015 event. The rainfall was not intense and long enough to result in high river levels and to trigger the operation of pumping stations. The records show that the water level at the WL gauge (Figure 9 (a)) increased rapidly right after the rainfall started, and reached to the peak level with a 15 minutes lag to the peak rainfall. This reflected the time of concentration at the node for collecting the surface runoff from its subcatchment. After the rainfall stopped, the water level gradually decreased because the coming discharge from further upstream pipes kept the water level high. Both Models A and B produced very similar changing trend but with 0.08m and 0.06m over-estimation of the peak level, respectively. For the water levels at the outlets, the outer water levels dropped below than the ones in pools such that pumping stations were not activated. The sewer flows were slowly discharged to the rivers by gravity, which was also reflected

in the slow declining water level at the WL gauge.

Table 2 show the NSEs of the modelled water level hydrographs, compared to the observations. Apart from the outlet of Network 2, which both models produced perfect predictions, Model B performed better than Model A for all locations. The reason for the perfect predictions was that the event was very short such that only limited observation records can be compared to.

Figure 10 compares the observation and modelled water level at the network outlets and the WL gauge of 23 July event. The WL gauge records show that the water level increased rapidly right after the rainfall started and stayed at a constant peak level because the full capacity of the network has been reached. The situation lasted for an hour because the coming discharge from further upstream pipes kept the water level high. Then the water level started to decrease, 30 minutes after the rainfall intensity has become lower than the design rainfall intensity. Figure 10 (a) shows that Model A has faster rising and declining limbs of the water level than Model B. It was due to that the flow response time in the gullies was not considered in Model A such that the surface water entered the sewer network more quickly. For the receding part, the water level in Model A began to decrease at eight minutes earlier than the observation, while the Model B result showed a slower timing and pace of water receding. It was due to that Model B was able to capture more surface water through gully inlets from the upstream catchments such that the water level maintained higher than Model A for longer.

The water levels at network outlets rapidly increased when the rainfall intensity was above the design rainfall. The operation of pumping station 1 quickly reduced the water level from 13:50. In general, the water level in Model B increased at a slower rate because the flow process in gullies was considered that the runoff collected

from inlets reached to the manhole later than the one in Model A, which assumes that the runoff moves from inlets to manhole immediately. This led to a slower rate of overland flow entering the sewer network, which resulted in later water level increase in the rising part of the hydrograph in sewer network, and a lower discharge of the surcharge flow downstream. Consequently, more water volume stayed in the sewer network such that the water level took longer time to recede, which can be observed in the water level hydrographs. For other networks, the pumps began operating around 13:20 because the continuous rainfall in previous 30 minutes has increased the water levels at the detention pools at WL gauge (a), at the outlet detention pools of Networks 1 to 4 (b-e, respectively).

Table 3 shows the NSEs of the modelled water level hydrographs, compared to the observations. Clearly, Model B performed better than Model A for all locations.

Although the pumping stations managed to cope with the flow concentrating to the outlets, the upstream pipes of the networks were unable to convey all inflow such that surcharge occurred, as discussed earlier about the condition at the WL gauge. Figure 11 and Figure 12 compare the modelled flood extents to the surveyed one, which was investigated by Taipei City Government after the event, for Model A and B, respectively. The field survey was carried out on the basis of road sections such that the flood extents were delineated along the roads, as a result, the mapped extent may be slightly inconsistent to the real flood situations. Unfortunately, there was no detailed flood depth information attached such that it was not possible to compare the modelled flood depth to the observation.

The flood extent in the subcatchments nearby the WL gauge in Model A was smaller than in Model B, but the simulated flood extents from both models were close to the surveyed one. The negligence of the flow process in gullies allowed overland flow to

enter the upstream manhole more easily such that the modelled flood extent was smaller in this area. Same situation occurred in the upstream area of Network 4 (i.e. the flood extent near the bottom boundary), where Model A simulated a smaller flood extent than Model B because the model setting collected more surface runoff from nearby region.

For Network 3, the increased upstream flow in Model A led to a greater flood extent along the main road in the east subcatchment. The long road spans the upstream subcatchments of four branches. The flooding in Model A was due to the surcharge water from the second bottom branch that the higher flow in the main trunk affected the runoff entering from this branch. The surcharged water propagated along the main road and flowed southward due to the terrain configuration. In Model B, the gullies could not drain the runoff in the northern part on the same road such that more flooding in that area was simulated. Nevertheless, it reduced the downstream pipe flow such that simulated flood extent in the midstream area in Model B was smaller than in Model A.

Table 4 shows the performance of Model A and Model B in predicting the overland flood extent. Both models predicted the flood conditions accurately with 98% of the case study area (Accuracy). However, if we narrow down the area to the surveyed flood extent, Model A only simulated 75% correctly, while Model B performed slightly better at 81% (Sensitivity). In terms of Precision, only 66% and 72% of flood area simulated by Model A and Model B, respectively, was actually flooded. In summary, Model B considered the flow processes in gullies, which enabled it to simulate the interactions between OFM and SFM better and produce results that were closer to the reality.

3.3.3 Modelling costs

For Model B, extra information regarding gullies were required for setting up. Such detailed data are often difficult or/and expensive to obtain, which is also the main reason why most modelling approaches ignore these elements. Luckily, in the study, we received the information from the Taipei City Government's field survey data. For areas where the surveyed data were absent, we adopted the City Government's storm sewer design standard to set up the inlets and gullies along the road sides in Model B.

Table 5 compares the computing time of both Models A and B running on the same desktop computer (with Intel i7-8700 3.7G CPU and 32GB RAM). As expected, Model B required more time for calculating the flow in gullies. Nevertheless, the extra 1D SFM computing cost was relatively small, comparing to the 2D OFM part, such that only 1.2 – 3.4% additional cost was incurred to provide better modelling results.

4 Conclusions

In this study, we proposed an improved Mixed OFM/SFM and SFM/OFM coupling approach for urban flood modelling by considering the flow process through gullies, which is often ignored in most OFM/SFM or SFM/OFM coupling approaches. Such detailed process may change the flow dynamic in sewer network and consequently affect the predictions of flood locations and extents. The proposed approach allows better description of the flow dynamic between overland and sewer system flows. The comparisons with the observed water level hydrographs and flood extent in the case study demonstrated that Models A and B can provide reliable modelling results for both moderate and extreme weather conditions, which allows flood risk managers to identify hotspots for developing mitigation measures.

Acknowledgment

The research is partially funded by the SINATRA project which is supported by the United Kingdom NERC Flooding from Intense Rainfall programme (grant NE/K008765/1). The data used in the study were provided by Taipei City Government, Taiwan, which will be available for reuse upon request and subjected to the approval of Taipei City Government.

References

Abbott, M.B., Minns, A.W., 1998. Computational Hydraulics, 2nd ed. Ashgate Publishing Limited, The Netherlands.

Allitt, R., Blanksby, J., Djordjević, S., Maksimović, C., Stewart, D., 2009. Investigations into 1D-1D and 1D-2D Urban Flood Modelling – UKWIR project. Presented at the WaPUG Autumn Conference 2009, Blackpool, UK.

Arnbjerg-Nielsen, K., 2008. Quantification of climate change on extreme precipitation used for design of sewer systems. Presented at the 11th International Conference on Urban Drainage.

Balmforth, D., Digman, C., Kellagher, R., Butler, D., 2006. Designing for exceedance in urban drainage – good practice (No. CIRIA C635). CIRIA.

Bazin, P., Nakagawa, H., Kawaike, K., Paquier, A., Mignot, E., 2014. Modeling Flow Exchanges between a Street and an Underground Drainage Pipe during Urban Floods. J. Hydraul. Eng. 04014051. https://doi.org/10.1061/(ASCE)HY.1943-7900.0000917

Bloomberg, M.R., Strickland, C.H., 2012. Guidelines for the Design and Construction of Stormwater Management Systems. N. Y. City Dep. Environ. Prot. Consult. N. Y. City Dep. Build. N. Y. NY USA.

BSI, 2008. Drain and sewer systems outside buildings - Part 4: Hydraulic design and environmental considerations. British Standards Institution.

Chang, T.-J., Wang, C.-H., Chen, A.S., 2015. A novel approach to model dynamic flow interactions between storm sewer system and overland surface for different land covers in urban areas. J. Hydrol. 524, 662–679. https://doi.org/10.1016/j.jhydrol.2015.03.014

Chen, A., Leandro, J., Djordjevic, S., 2016. Modelling sewer discharge via displacement of manhole covers during flood events using 1D/2D SIPSON/P-DWave dual drainage simulations. Urban Water J. 13, 830–840. https://doi.org/10.1080/1573062X.2015.1041991

Chen, A.S., Djordjević, S., Leandro, J., Savic, D., 2007. The urban inundation model with bidirectional flow interaction between 2D overland surface and 1D sewer networks. Presented at the NOVATECH 2007, Lyon, France, pp. 465–472.

CIWEM UDG, 2016. Rainfall Modelling Guide 2016. CIWEM, London.

Djordjević, S., Prodanović, D., Maksimović, C., 1999. An approach to stimulation of dual drainage. Wat Sci Tech 39, 95–103.

Djordjević, S., Saul, A.J., Tabor, G.R., Blanksby, J., Galambos, I., Sabtu, N., Sailor, G., 2012. Experimental and numerical investigation of interactions between above and below ground drainage systems. Water Sci. Technol. 67, 535. https://doi.org/10.2166/wst.2012.570

Gomez, M., Recasens, J., Russo, B., Martinez-Gomariz, E., 2016. Assessment of inlet efficiency through a 3D simulation: numerical and experimental comparison. Water Sci. Technol. 74, 1926–1935. https://doi.org/10.2166/wst.2016.326

Hsu, M.H., Chen, S.H., Chang, T.J., 2002. Dynamic inundation simulation of storm water interaction between sewer system and overland flows. J. Chin. Inst. Eng. 25, 171–177.

Hsu, M.H., Chen, S.H., Chang, T.J., 2000. Inundation simulation for urban drainage basin with storm sewer system. J. Hydrol. 234, 21–37. https://doi.org/10.1016/S0022-1694(00)00237-7

Huber, W.C., Dickinson, R.E., 1988. Storm Water Management Model. User's Manual Ver. IV. U. S. Environmental Protection Agency., Athens Georgia, U.S.A.

Jahanbazi, M., Egger, U., 2014. Application and comparison of two different dual drainage models to assess urban flooding. Urban Water J. 11, 584–595. https://doi.org/10.1080/1573062X.2013.871041

Leandro, J., Chen, A.S., Djordjević, S., Savic, D.A., 2009. Comparison of 1D/1D and 1D/2D Coupled (Sewer/Surface) Hydraulic Models for Urban Flood Simulation. J. Hydraul. Eng. 135, 495–504. https://doi.org/10.1061/(ASCE)HY.1943-7900.0000037

Leandro, J., Martins, R., 2016. A methodology for linking 2D overland flow models with the sewer network model SWMM 5.1 based on dynamic link libraries. Water Sci. Technol. 73, 3017. https://doi.org/10.2166/wst.2016.171

Lopes, P., Leandro, J., Carvalho, R.F., Russo, B., Gómez, M., 2016. Assessment of the Ability of a Volume of Fluid Model to Reproduce the Efficiency of a Continuous Transverse Gully with Grate. J. Irrig. Drain. Eng. 142, 04016039. https://doi.org/10.1061/(ASCE)IR.1943-4774.0001058

Martins, R., Leandro, J., Chen, A.S., Djordjević, S., 2017. A comparison of three dual drainage models: Shallow Water vs Local Inertial vs Diffusive Wave. J. Hydroinformatics 10, 331–348. https://doi.org/10.2166/hydro.2017.075

Martins, R., Leandro, J., de Carvalho, R.F., 2014. Characterization of the hydraulic performance of a gully under drainage conditions. Water Sci. Technol. 69, 2423. https://doi.org/10.2166/wst.2014.168

Mays, L.W., 2011. Water resources engineering. John Wiley, Hoboken, NJ.

Nash, J.E., Sutcliffe, J.V., 1970. River flow forecasting through conceptual models part I — A discussion of principles. J. Hydrol. 10, 282–290. https://doi.org/10.1016/0022-1694(70)90255-6

Rossman, L.A., 2010. Storm water management model: User's manual Version 5.0.

466 Russo, B., Sunyer, D., Velasco, M., Djordjević, S., 2015. Analysis of extreme
467 flooding events through a calibrated 1D/2D coupled model: the case of
468 Barcelona (Spain). J. Hydroinformatics 17, 473.
469 https://doi.org/10.2166/hydro.2014.063

470 Seyoum, S.D., Vojinovic, Z., Price, R.K., Weesakul, S., 2012. Coupled 1D and
471 Noninertia 2D Flood Inundation Model for Simulation of Urban Flooding. J.
472 Hydraul. Eng.-Asce 138, 23–34. https://doi.org/10.1061/(Asce)Hy.1943-
473 7900.0000485

474 Shepherd, W., Blanksby, J., Doncaster, S., Poole, T., 2012. Assessment of Road
475 Gullies, in: Proceedings of 10th International Conference on Hydroinformatics.
476 Presented at the 10th HIC, Hamburg, Germany.

477 Vojinovic, Z., Tutulic, D., 2009. On the use of 1D and coupled 1D-2D modelling
478 approaches for assessment of flood damage in urban areas. Urban Water J.
479 6, 183–199. https://doi.org/10.1080/15730620802566877

480

Figures

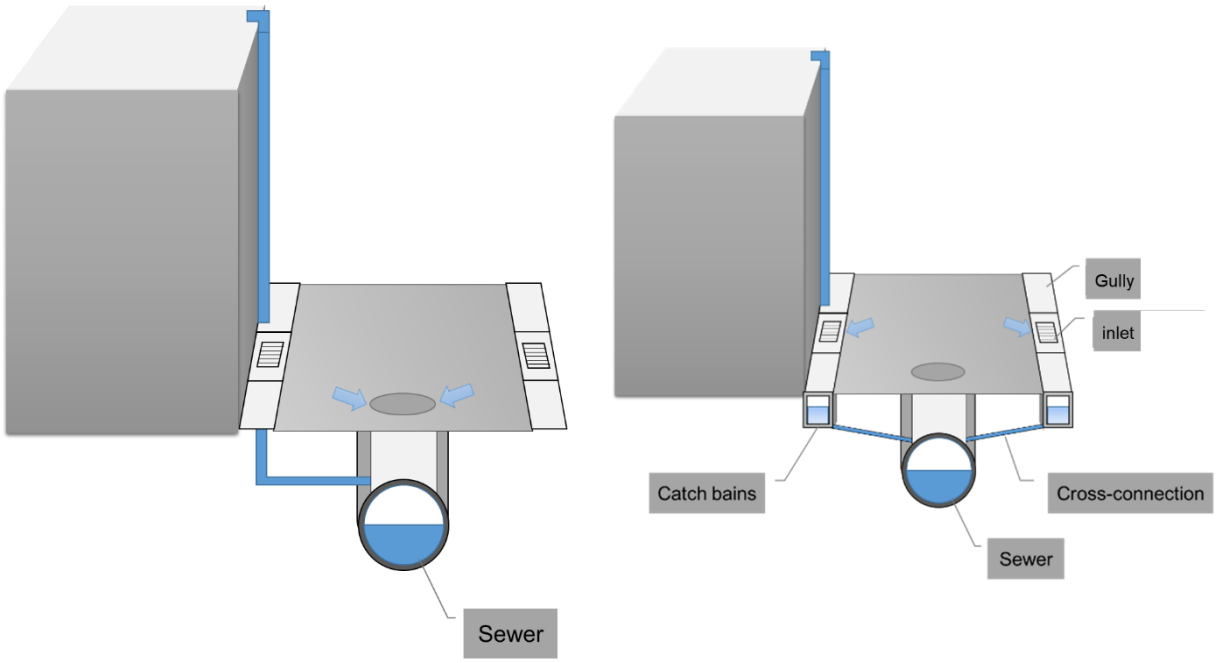

(a) (b)

Figure 1 Schematic representation of the interaction between 2D OFM and 1D SFM in (a) Model A without gullies (b) Model B with inlets and gullies

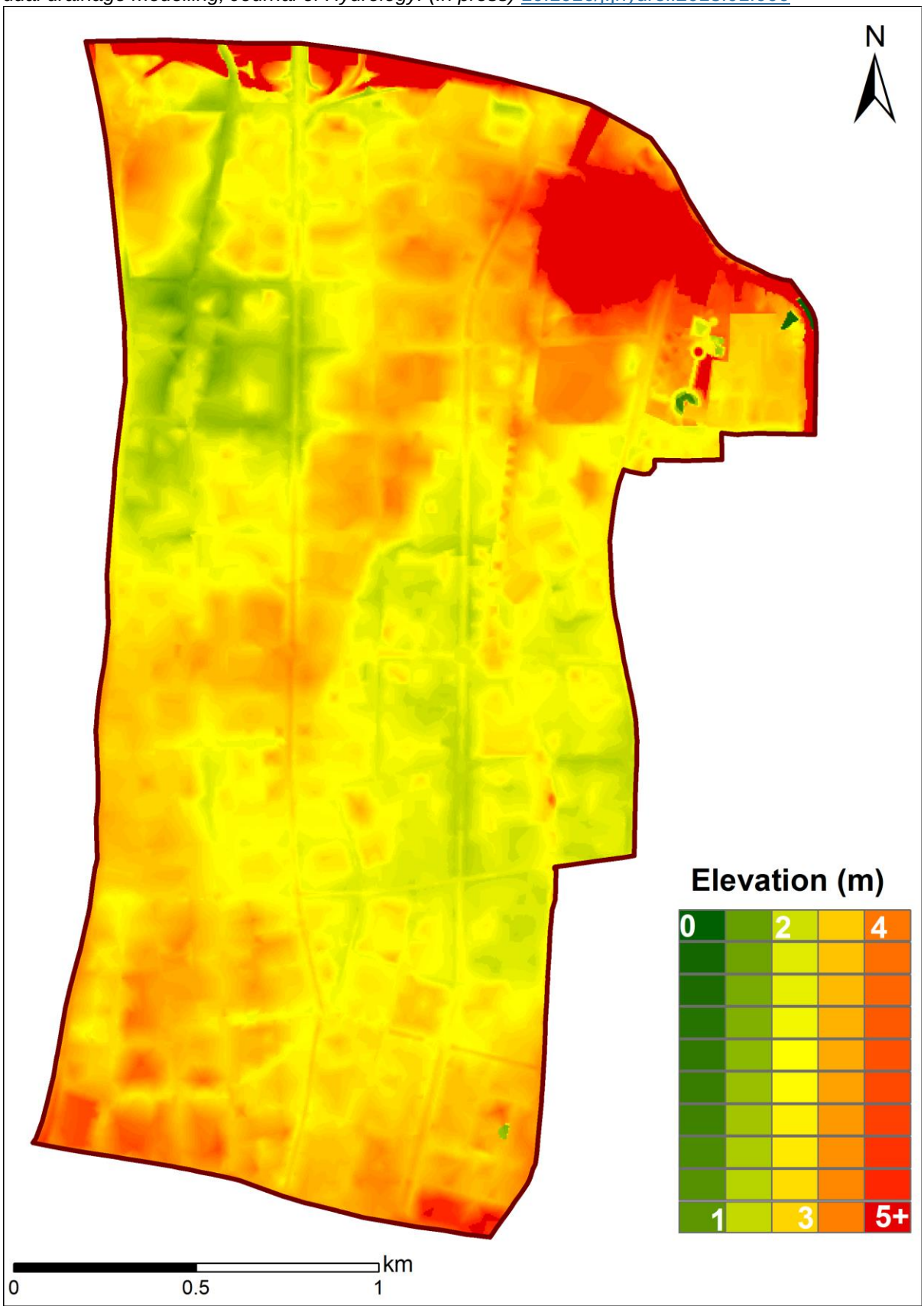

Figure 2 Terrain elevation of the case study area

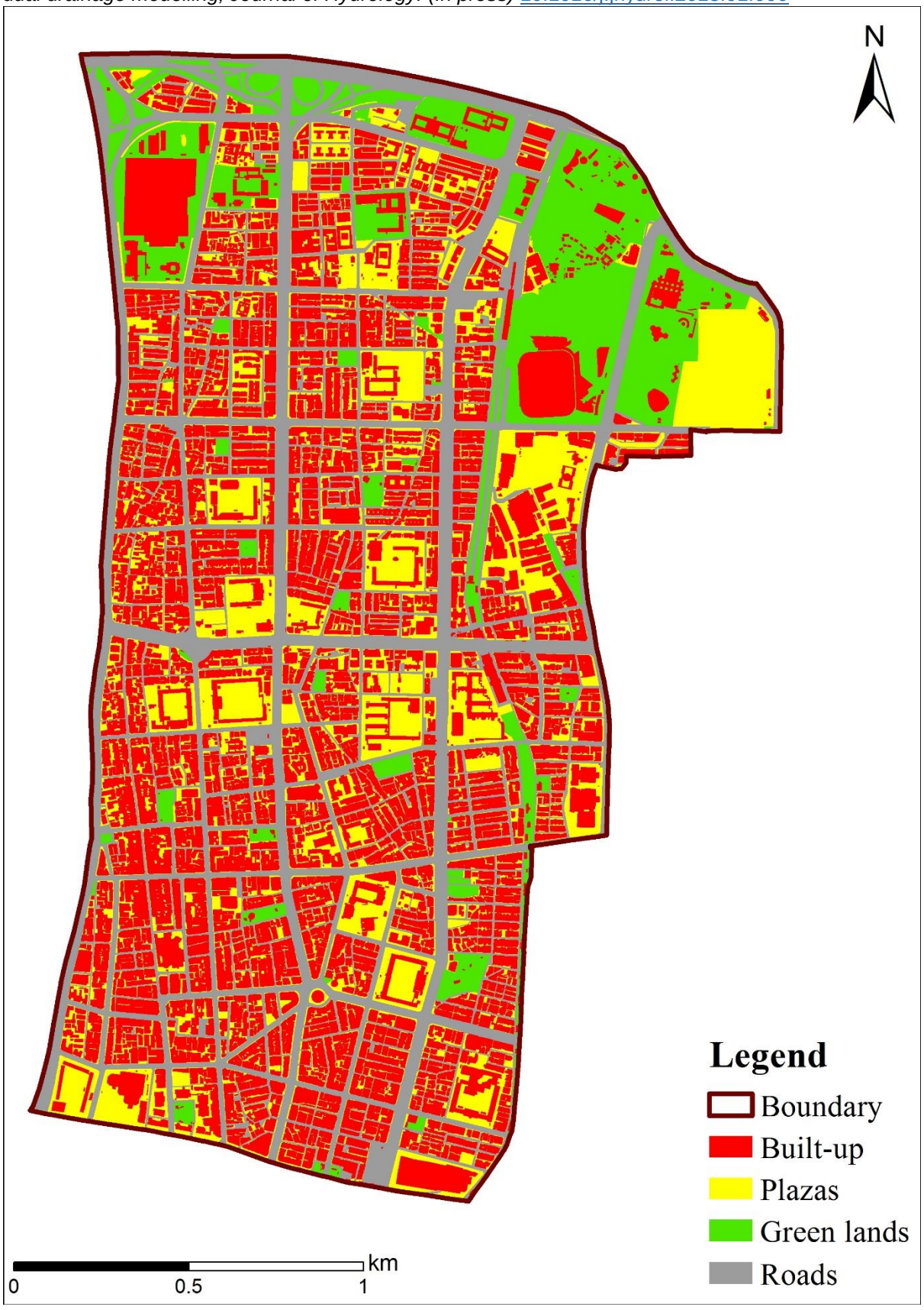

Figure 3 Land cover in the case study area

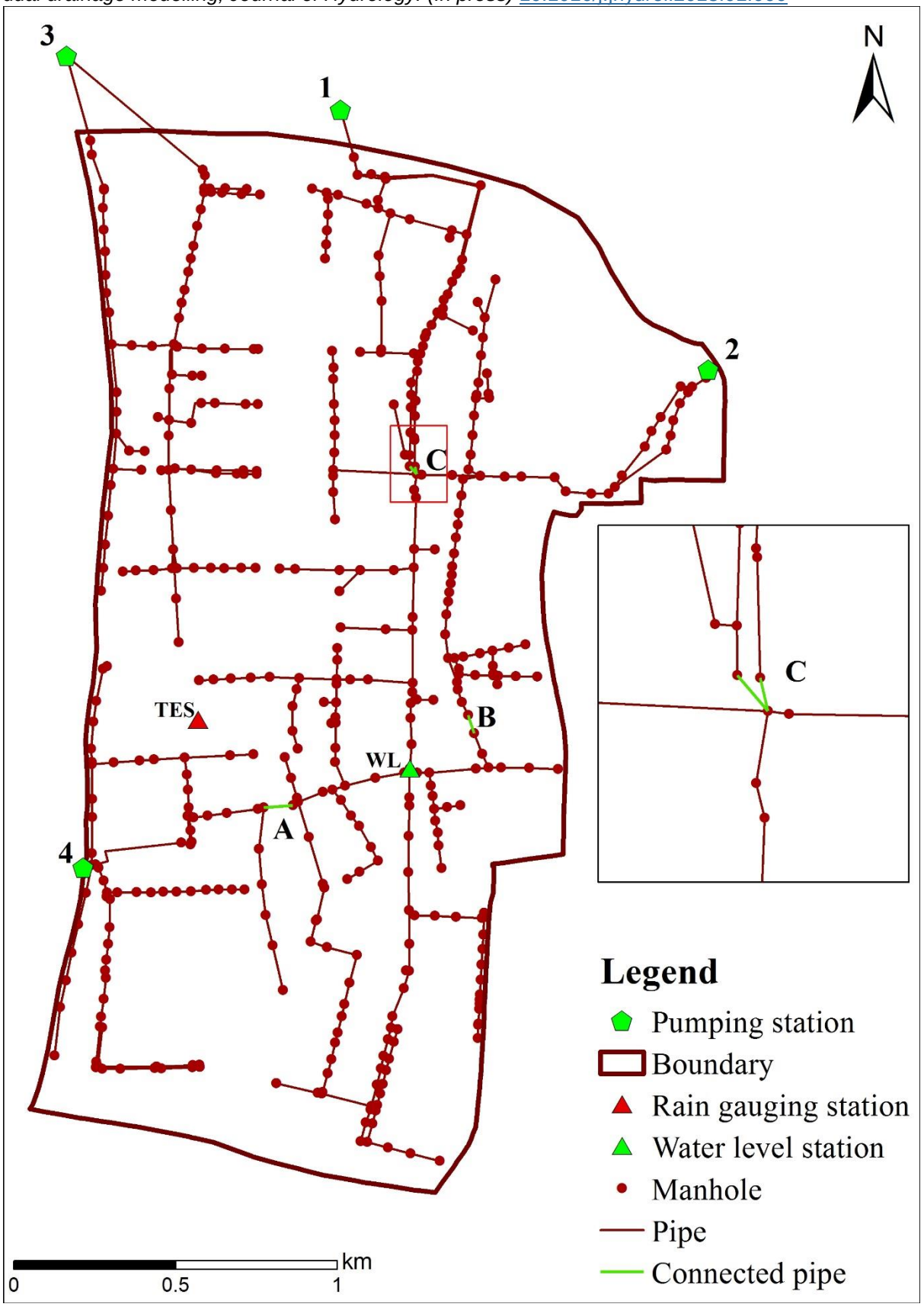

Figure 4 The drainage network and the locations of the TES rain gauge and the water level (WL) gauge in the case study area

Please cite: *Chang T-J, Wang C-H, Chen AS, Djordjevic S (2018) The effect of inclusion of inlets in dual drainage modelling, Journal of Hydrology. (In press)* 10.1016/j.jhydrol.2018.01.066

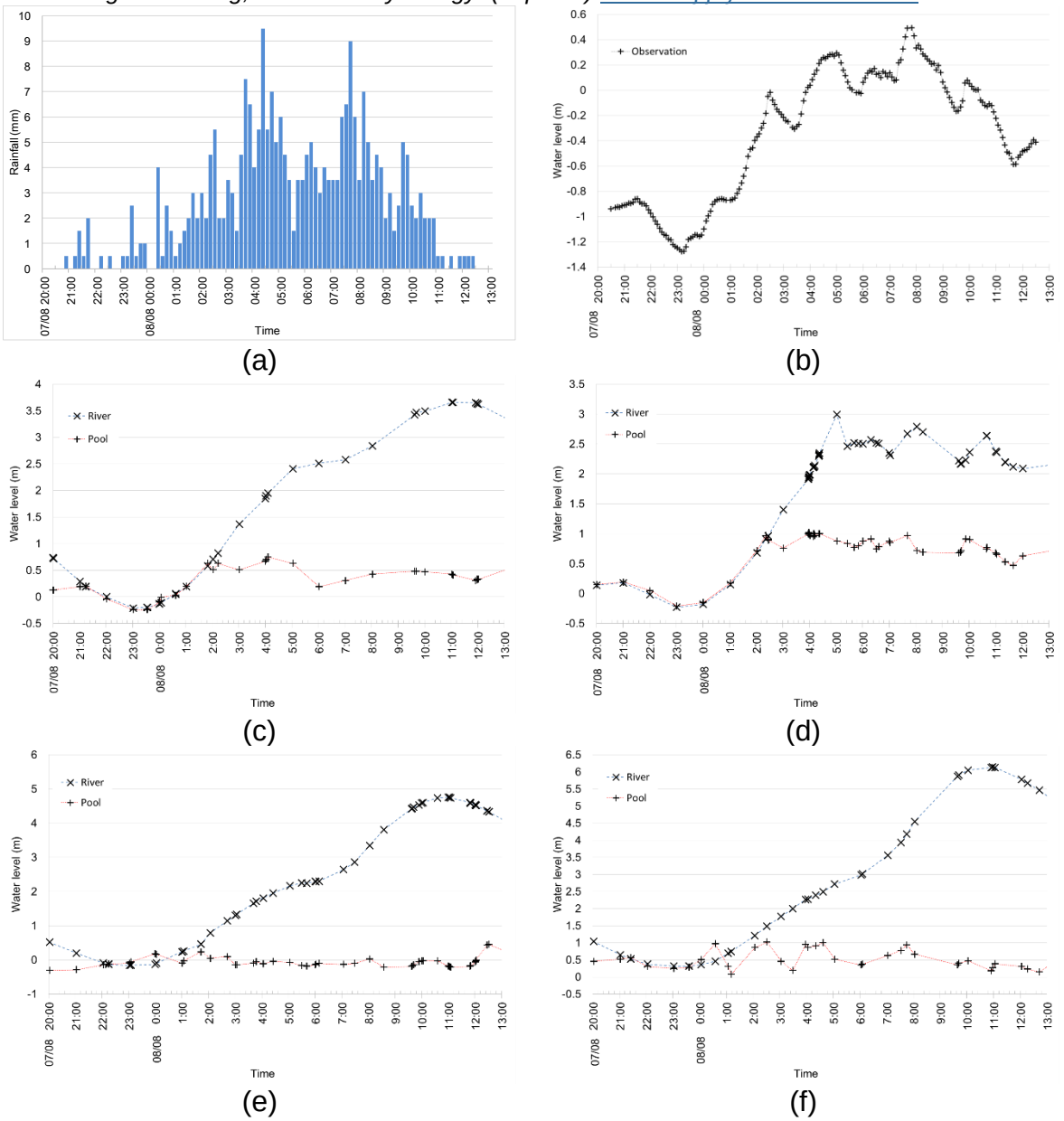

Figure 5 (a) The rainfall record at TES rain gauge; and the outer (river) and the inner (pool) inner and water level hydrographs at (b) at WL gauge; and (c-f) the outlet detention pools of Networks 1 to 4, respectively, of 7-8 August 2015 event.

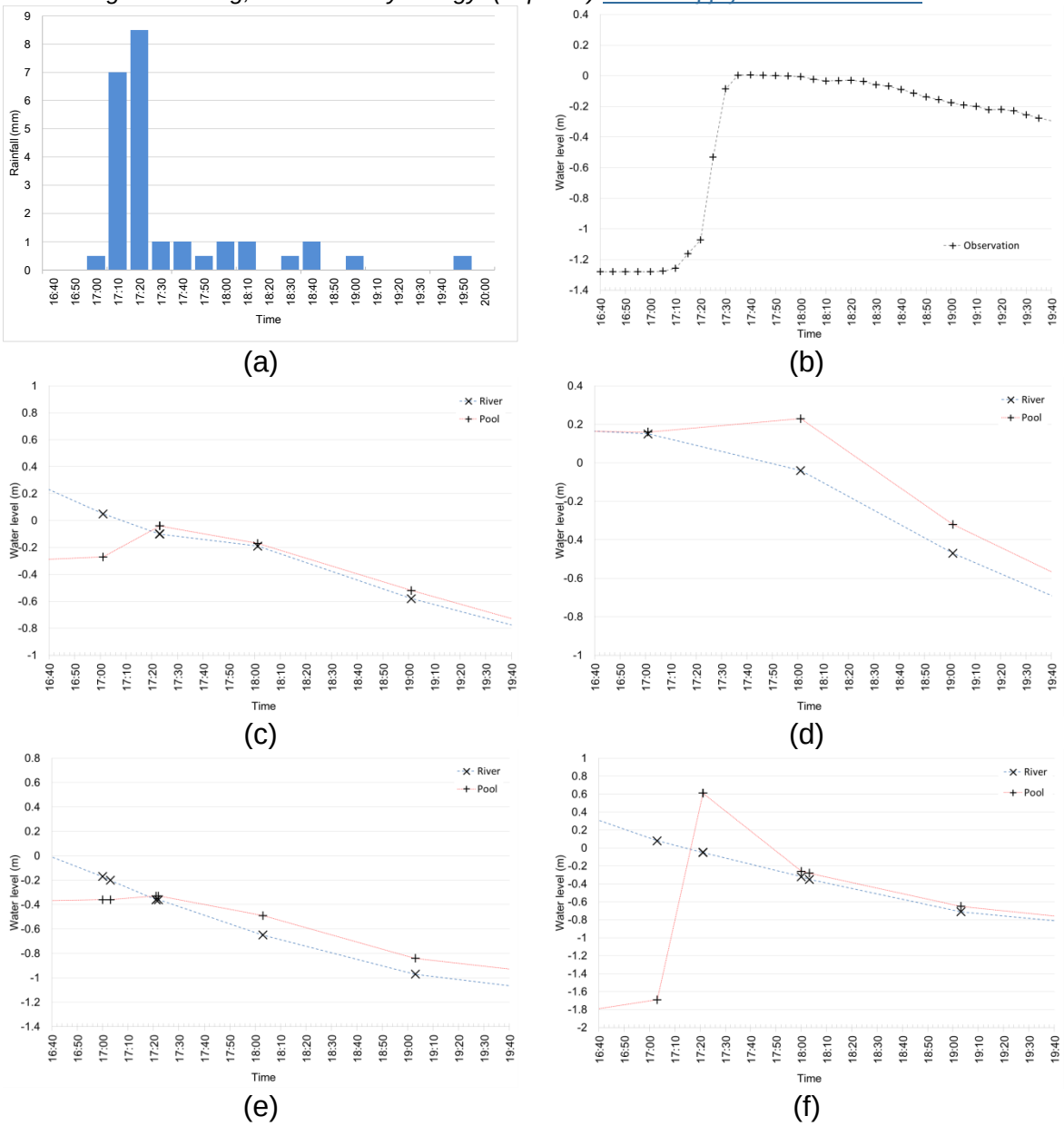

Figure 6 The rainfall record at TES rain gauge; and the outer (river) and the inner (pool) inner and water level hydrographs at (b) at WL gauge; and (c-f) the outlet detention pools of Networks 1 to 4, respectively, of 19 July 2015 event.

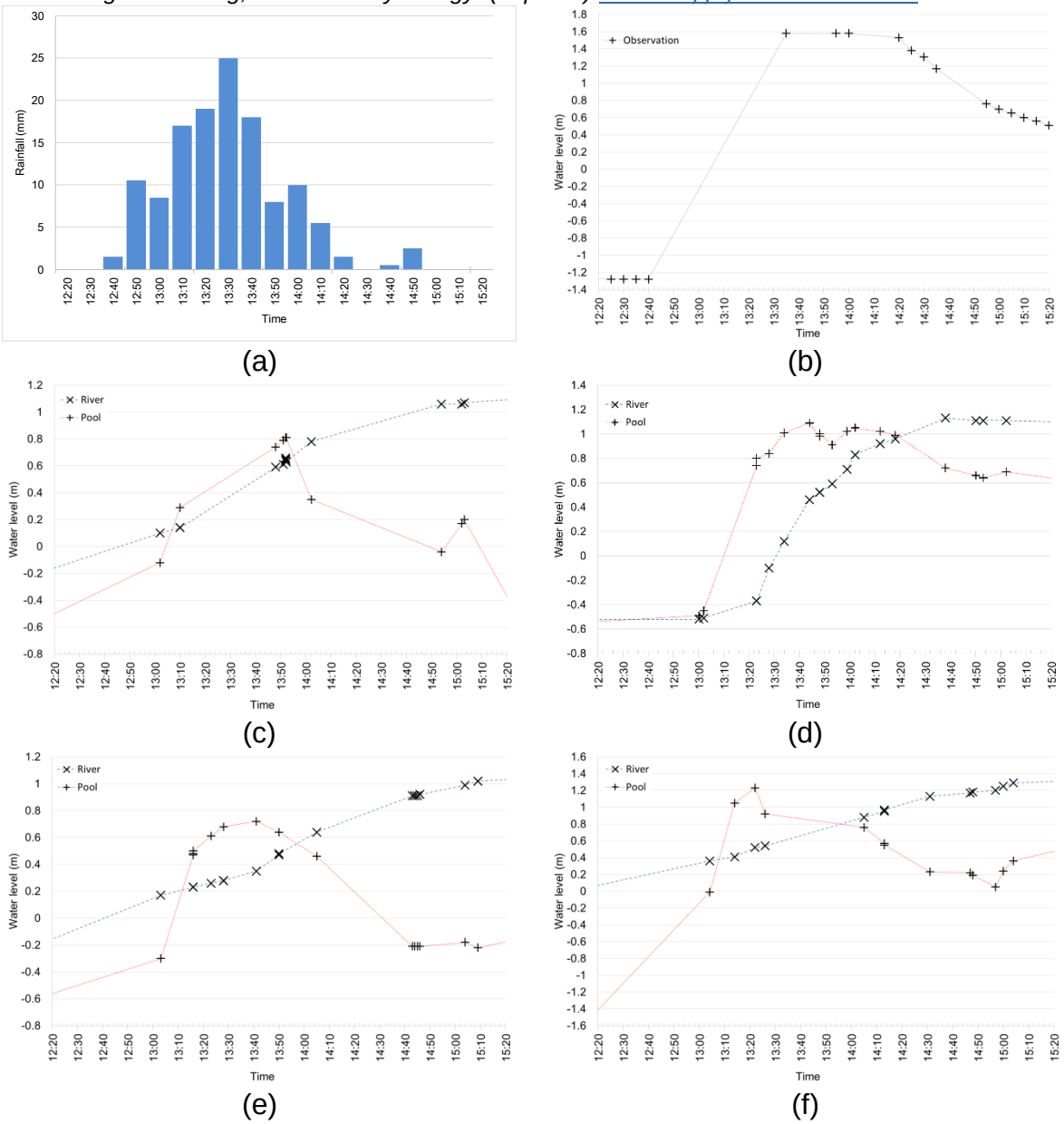

499 Figure 7 The rainfall record at TES rain gauge; and the outer (river) and the inner

500 (pool) inner and water level hydrographs at (b) at WL gauge; and (c-f) the outlet

501 detention pools of Networks 1 to 4, respectively, of 23 July 2015 event.

502

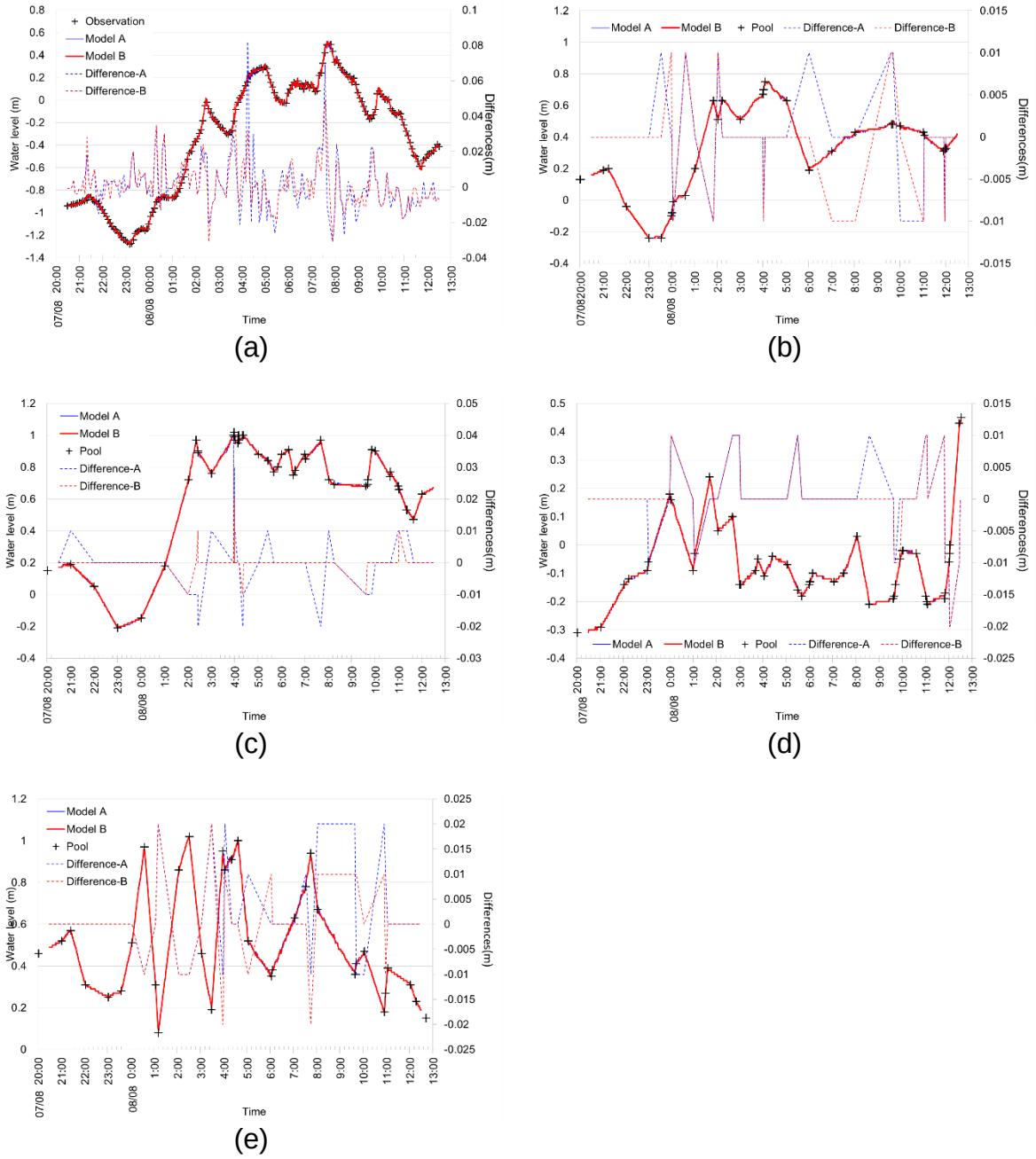

503 Figure 8 Observed and modelled water level hydrographs of the 7-8 August 2015
504 event at (a) WL gauge; and (b-e) the outlet detention pools of Networks 1 to 4 (b-e,
505 respectively).

506

507

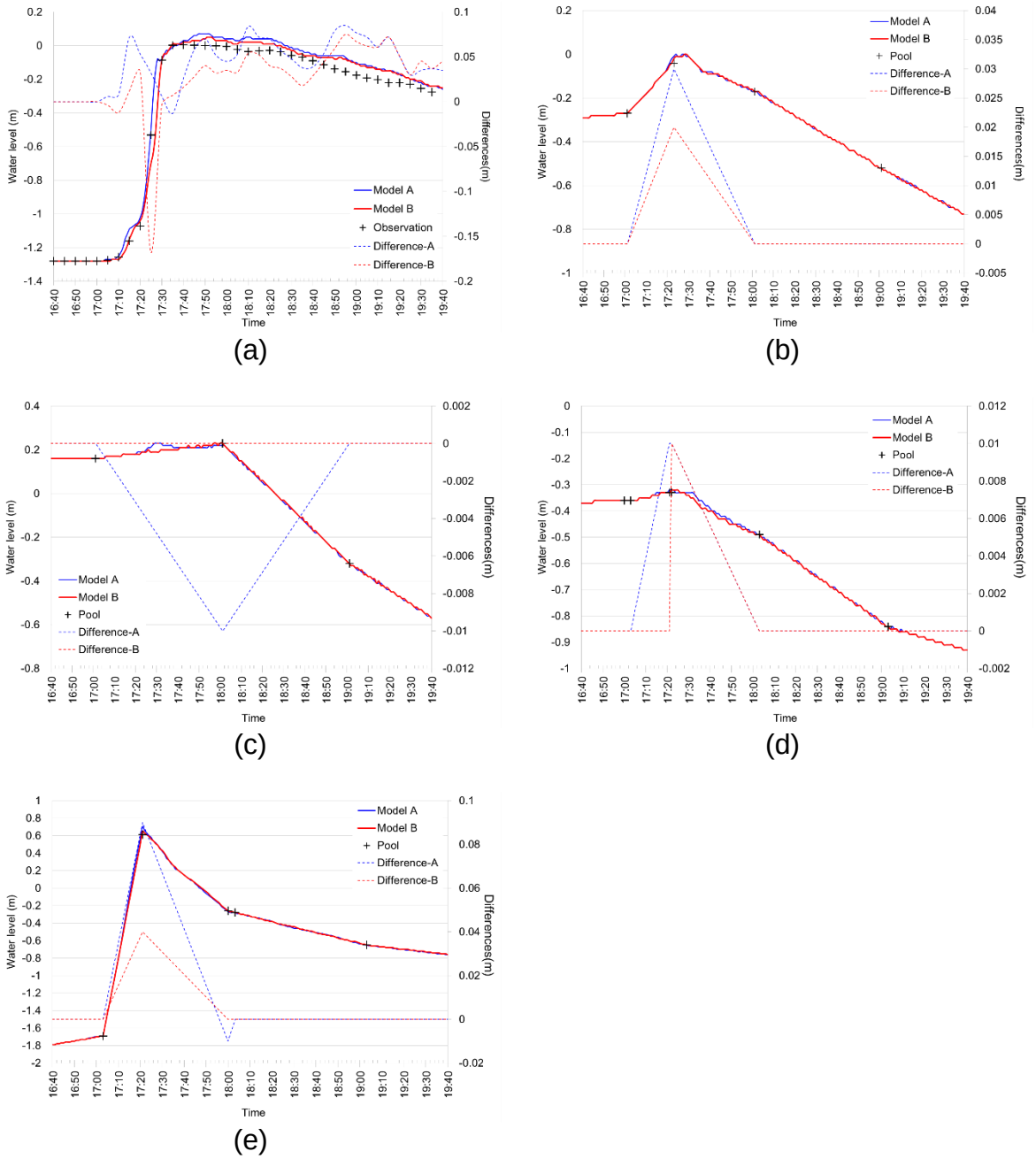

508 Figure 9 Observed and modelled water level hydrographs of the 19 July 2015 event

509 at WL gauge (a), at the outlet detention pools of Networks 1 to 4 (b-e, respectively).

510

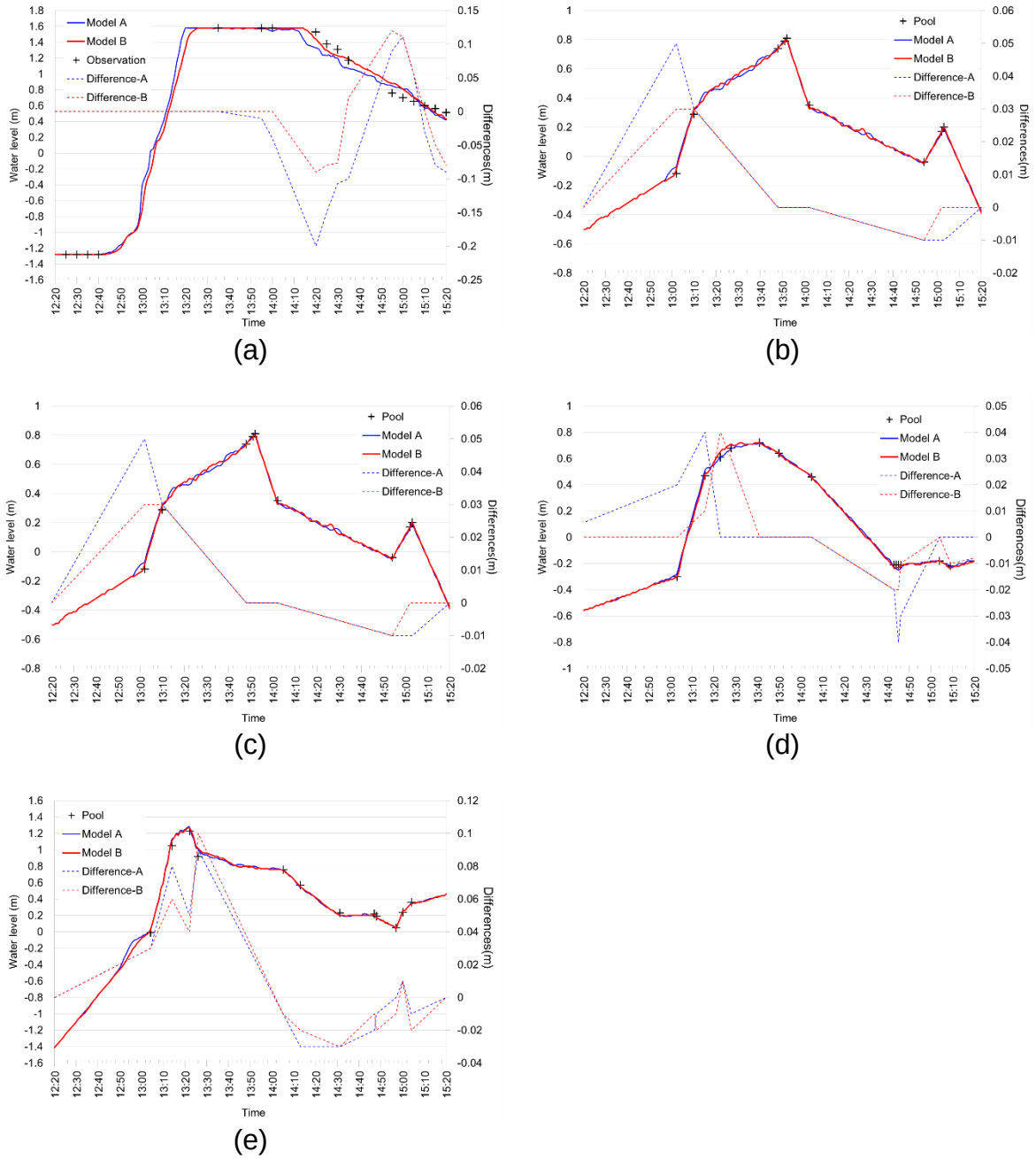

511 Figure 10 Observed and modelled water level hydrographs of the 23 July 2015 event

512 at WL gauge (a), at the outlet detention pools of Networks 1 to 4 (b-e, respectively).

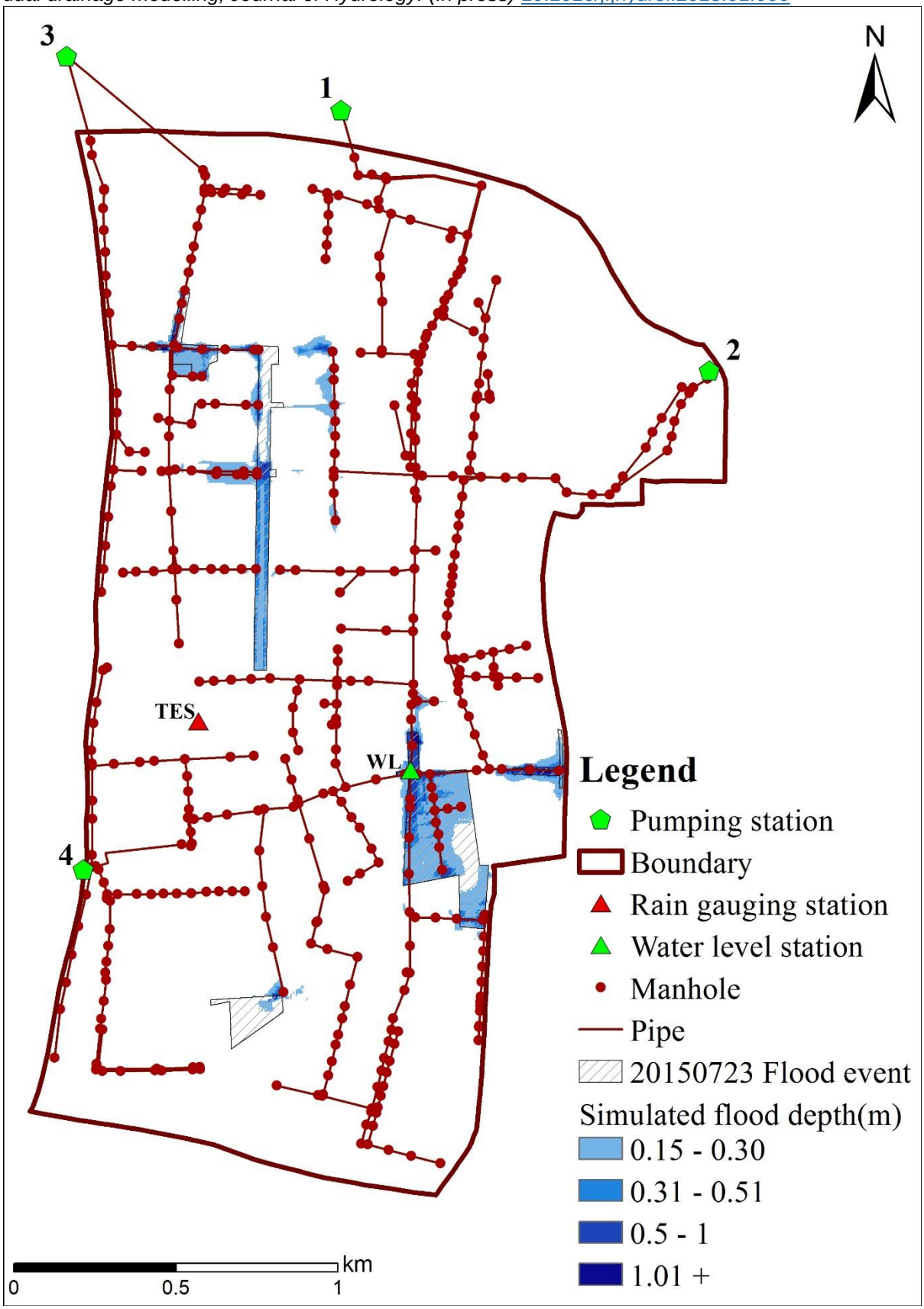

513

514 Figure 11 Comparison of surveyed and modelled flood extent (Model A) of the 23

515 July 2015 event

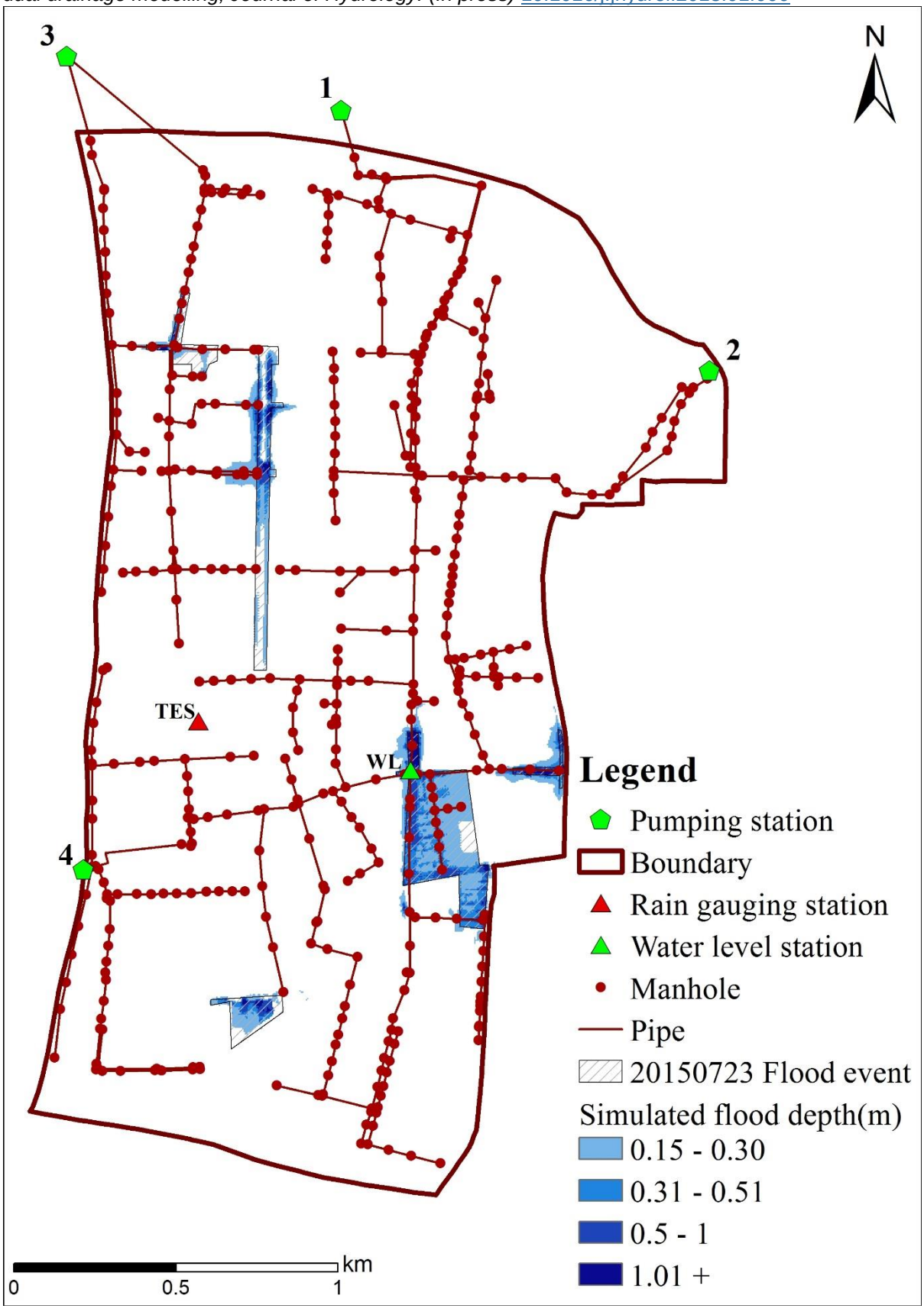

516

517 Figure 12 Comparison of surveyed and modelled flood extent (Model B) of the 23

518 July 2015 event

Please cite: *Chang T-J, Wang C-H, Chen AS, Djordjevic S (2018) The effect of inclusion of inlets in dual drainage modelling, Journal of Hydrology. (In press)* 10.1016/j.jhydrol.2018.01.066

519 **Table captions**

520 Table 1 The NSE of modelled water levels at the network outlets and WL gauge for

521 the 7-8 August 2015 event

Location	Model A	Model B
Network 1 outlet	0.9995	0.9995
Network 2 outlet	0.9991	0.9999
Network 3 outlet	0.9967	0.9968
Network 4 outlet	0.9986	0.9989
WL gauge	0.9992	0.9994

522

523 Table 2 The NSE of modelled water levels at the network outlets and WL gauge for

524 19 July 2015 event

Location	Model A	Model B
Network 1 outlet	0.9927	0.9968
Network 2 outlet	0.9994	1.0000
Network 3 outlet	0.9990	0.9995
Network 4 outlet	0.9970	0.9994
WL gauge	0.9894	0.9907

525

526 Table 3 The NSE of modelled water levels at the network outlets and WL gauge for

527 23 July 2015 event

Location	Model A	Model B
Network 1 outlet	0.9961	0.9976
Network 2 outlet	0.9978	0.9992
Network 3 outlet	0.9981	0.9981
Network 4 outlet	0.9891	0.9901
WL gauge	0.9944	0.9973

528

529 Table 4 The modelling performance indicators

Indicator	Model A	Model B
Accuracy	97.7%	98.1%
Sensitivity	75.1%	81.0%
Precision	65.8%	71.5%

530

531

Please cite: *Chang T-J, Wang C-H, Chen AS, Djordjevic S (2018) The effect of inclusion of inlets in dual drainage modelling, Journal of Hydrology. (In press)* 10.1016/j.jhydrol.2018.01.066

532

533 Table 5 The comparison of computing time)

Event	Computing time (s)		Ratio
	Model A	Model B	(Model B / Model A)
7-8 August 2015	13.594	13,753	1.012
19 July 2015	2,267	2,302	1.015
23 July 2015	2,586	2,674	1.034

534